PROCEEDINGS OF SCIENCE

ALPs as dark matter mediators: beyond freeze-out

Aoife Bharucha[a,*] **and Sophie Mutzel**[a]

[a] *Aix Marseille Univ, Université de Toulon, CNRS, CPT, IPhU, Marseille, France*

E-mail: aoife.bharucha@cpt.univ-mrs.fr, sophie.mutzel@cpt.univ-mrs.fr

Recent experimental advances now severely constrain electroweak-scale WIMPs produced via thermal freeze-out, leading to a shift away from this standard paradigm. Here we consider an axion-like particle (ALP), the pseudo-Goldstone boson of an approximate U(1) global symmetry spontaneously broken at a high scale f_a, as a mediator between the Standard Model (SM) particles and the dark matter (DM) particles. We explore the case where the couplings are too small to allow for DM generation via freeze-out and the mediator particle and the DM constitute a hidden sector which is thermally decoupled from the SM particles. However, alternative generation mechanisms such as freeze-in and decoupled freeze-out are now appropriate. Having determined the region of parameter space where the correct relic density is obtained, we then revisit experimental constraints on ALPs from electron beam dump experiments, astrophysics and rare B and K decays.

8th Symposium on Prospects in the Physics of Discrete Symmetries (DISCRETE 2022)
7-11 November, 2022
Baden-Baden, Germany

*Speaker

PoS(DISCRETE2022)023

1. Introduction

Increasing constraints on the WIMP paradigm bring the dark matter (DM) genesis mechanism into question. We wish to study alternative generation mechanisms for the case of an axion-like particle (ALP) acting as a mediator to DM. It has been shown in ref. [3] that in the parameter space of a light DM mediator, there are several possibilities beyond freeze-out, and these cover a large and continuous region in the ALP couplings to the SM and the DM. All these possibilities depend on the dark sector not being in equilibrium with the SM at the time of reheating. One well known example is freeze-in, where the DM is slowly produced from the thermal bath, but never reaches equilibrium with the mediator or the SM, see e.g. [6]. Another idea was put forward in ref. [3], that for certain couplings, before the DM decouples it could enter into equilibrium with the mediator at a temperature distinct from that of the thermal bath. These two fascinating scenarios are presented here.

2. The Model

If a new light pseudoscalar a exists, it might well be an axion-like particle (ALP), i.e. the pseudo-Goldstone boson of an approximate $\mathrm{U}(1)_{\mathrm{PQ}}$ global symmetry, spontaneously broken at a high scale f_a ($\Rightarrow$ light). Such an ALP could act as a mediator between the SM fermions (f) and the dark matter (χ), a $\mathrm{U}(1)_{\mathrm{PQ}}$ charged Dirac fermion. In our model, below the electroweak scale the ALP only couples at tree level to SM fermions via Yukawa-like interactions, interactions with gauge and Higgs bosons are via fermion loops. If the fermion content is purely SM-like, the anomaly cancellation requirement implies that the contributions from dimension-5 terms cancel to leave only dimension-4, mass-dependent terms [1]. However, as the ALP can emerge naturally from an extended Higgs sector, the dimension-5 coupling between Higgs, ALP and SM fermions must also be taken into account. We hence consider the following relevant new terms in the effective Lagrangian (below the electroweak symmetry breaking scale):

$$\begin{aligned}\mathcal{L} \supset & \frac{1}{2}\partial_\mu a \partial^\mu a + \bar{\chi}(i\partial\!\!\!/ - m_\chi)\chi - \frac{1}{2}m_a^2 a^2 + ia\sum_f \frac{m_f}{f_a} C_f \bar{f}\gamma_5 f \\ & + ia\frac{m_\chi}{f_a} C_\chi \bar{\chi}\gamma_5\chi + a\sum_f C_f \frac{y_f}{\sqrt{2}f_a}\, h\, \bar{f} i\gamma_5 f + \ldots \end{aligned} \tag{1}$$

Here, f is any Standard Model fermion with mass m_f, the masses of the χ and of the ALP are m_χ and m_a, and C_f and C_χ are the dimensionless couplings between the ALP and the SM fermions and DM respectively. In the following we will however work with the redefined couplings: $g_{a\chi\chi} \equiv m_\chi C_\chi / f_a$ will be referred to as the *hidden sector coupling* and $g_{aff} \equiv C_f / f_a$ as the *connector coupling*. Note that there is no ALP coupling to gauge bosons at tree-level but of course this may arise via loops.

Note that if a was the (DFSZ-like) QCD axion, multiple astrophysical and laboratory constraints would apply (see [5] for overview), although it may be possible to circumvent these constraints by extensive model-building. Therefore we assume that the a mass is mainly due to some explicitly $\mathrm{U}(1)_{\mathrm{PQ}}$-breaking effect other than the anomaly, which allows us to consider m_a and g_{aff} independently and as a result evade constraints.

3. Dark matter generation beyond freeze-out

As the scale f_a should be large, the couplings are in general too small to give the correct relic density through freeze-out. An alternative to the standard freeze-out scenario is that the initial abundances of the dark sector particles, i.e. the DM and the ALP, are negligible compared to the SM thermal bath after reheating, and they do not reach equilibrium with the SM before decoupling. For example, in the freeze-in mechanism: the dark sector particles are gradually produced by scattering processes in the thermal plasma without reaching equilibrium, until the temperature decreases enough that the processes decouple and the DM abundance remains constant (see e.g. [6]). Note that there are two possibilities, IR freeze-in where the final relic density is insensitive to the reheating temperature, or UV freeze where the choice of reheating temperature influences the result, depending on the T dependence of the thermal cross section. In our work we concentrate on the following mechanisms:

- For the case of small $g_{a\chi\chi}$ and g_{aff}, the DM is produced via freeze-in. Either, when $T_{RH} \lesssim 1$ TeV directly via $f\bar{f} \to \chi\bar{\chi}$ or, for example, $f\bar{f} \to ag$ followed by $aa \to \chi\bar{\chi}$, where the ALP may or may not be in equilibrium with the SM [7]. Alternatively, for larger T_{RH}, the dominant contribution comes from UV freeze-in via the 2→3 scattering process $f\bar{f} \to h\chi\bar{\chi}$ as well as $f\bar{f} \to ha$ followed by $aa \to \chi\bar{\chi}$.
- At intermediate g_{aff}, the ALPs do not reach equilibrium with the SM particles, but if $g_{a\chi\chi}$ is sufficiently large, the ALPs and DM particles may enter into equilibrium, leading to freeze-out from a thermally decoupled dark sector, or to put it simply, decoupled freeze-out (DFO), see [3], and more recently [4].

Let's study how to solve the Boltzmann equations in these different cases.

Taking into account the interactions between the SM, DM particles and the ALPs in eq. 1 we can write down the most general, complete set of coupled differential equations governing the evolution of the number densities of the a and χ, n_a and n_χ respectively:

$$\begin{aligned}
\frac{\mathrm{d}n_\chi}{\mathrm{d}t} + 3Hn_\chi &= \sum_f \left\langle \sigma_{\chi\bar{\chi}\to f\bar{f}} v \right\rangle \left(\left(n_\chi^{\mathrm{eq}}\right)^2 - n_\chi^2 \right) + \left\langle \sigma_{aa\to\chi\bar{\chi}} v \right\rangle n_a^2 - \left\langle \sigma_{\chi\bar{\chi}\to aa} v \right\rangle n_\chi^2 \\
&\quad + \sum_{i,j,k} \left(\left\langle \sigma_{\chi\bar{\chi}\to ijk} v \right\rangle \left(\left(n_\chi^{\mathrm{eq}}\right)^2 - n_\chi^2 \right) + \left\langle \sigma_{\chi\bar{\chi} i\to jk} v^2 \right\rangle n_i^{\mathrm{eq}} \left(\left(n_\chi^{\mathrm{eq}}\right)^2 - n_\chi^2 \right) \right) , \\
\frac{\mathrm{d}n_a}{\mathrm{d}t} + 3Hn_a &= \sum_{i,j,k} \left\langle \sigma_{ia\to jk} v \right\rangle \left(n_a^{\mathrm{eq}} n_i^{\mathrm{eq}} - n_a n_i^{\mathrm{eq}} \right) + \left\langle \Gamma_a \right\rangle \left(n_a^{\mathrm{eq}} - n_a \right) \\
&\quad - \left\langle \sigma_{aa\to\chi\bar{\chi}} v \right\rangle n_a^2 + \left\langle \sigma_{\chi\bar{\chi}\to aa} v \right\rangle n_\chi^2 \, .
\end{aligned} \tag{2}$$

Here i, j, k are SM particles which are involved in the relevant processes (the dominant contribution coming from the t-channel process $i = g$, $j = \bar{k} = t$). The $2 \to 2$ or $2 \to 3$ processes enter via the typical thermally averaged cross section $\langle \sigma v \rangle$ and the (inverse) decay of the pseudoscalar via the thermally averaged decay rate, $\langle \Gamma_a \rangle$ [2]. We have applied the principle of detailed balance where appropriate.

Solving these equations within the chosen range of hidden sector and connector couplings, for fixed masses $m_\chi = 10$ GeV and $m_a = 1$ GeV, results in the phase diagram in figure 1. Note

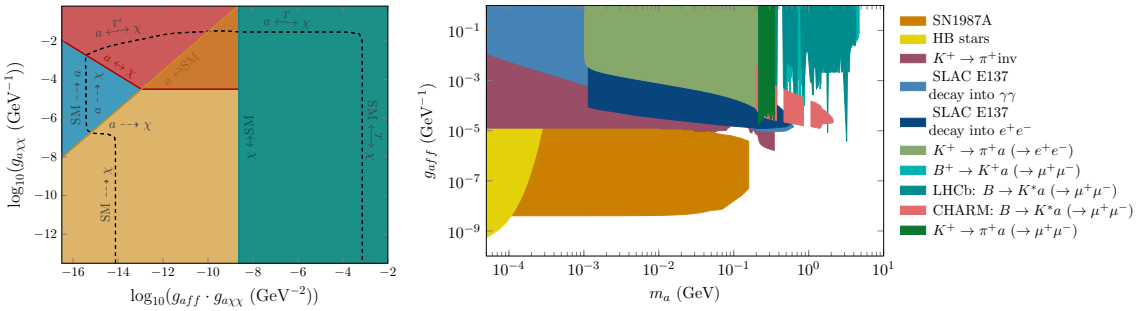

Figure 1: Left: ALP-DM coupling $g_{a\chi\chi}$ as a function of the product of the ALP-DM and the ALP-fermion coupling, $g_{a\chi\chi} \cdot g_{aff}$, for $m_\chi = 10$ GeV and $m_a = 1$ GeV. The dashed line corresponds to the combination of couplings which give the correct DM relic density $\Omega_{\mathrm{DM}}h^2 = 0.12$ as measured by the Planck telescope. Right: Full constraint plot on the ALP-fermion coupling g_{aff} as a function of the ALP mass m_a for an ALP which only couples to SM fermions at tree level.

that the dashed line indicates the couplings giving rise to the observed DM relic density. As first shown in [3] and later shown in [4] for the case of the dark photon, the massive mediator case leads to five different mechanisms of DM generation. Let us discuss each of these briefly. In the lower left (yellow) region of figure 1, i.e. for small $g_{a\chi\chi}$ and $g_{aff} \cdot g_{a\chi\chi}$, the DM particles are not in equilibrium with the SM particles or the ALPs, but the ALP fermion coupling is large enough for the ALPs and the SM to reach equilibrium. When the DM is produced directly from collisions of SM fermions, $f\bar{f} \to \chi\bar{\chi}$, we call it *freeze-in from the SM*. On increasing $g_{a\chi\chi}$ while keeping the product $g_{aff} \cdot g_{a\chi\chi}$ fixed, $aa \dashrightarrow \chi\bar{\chi}$ becomes the dominant process; this is *freeze-in from the mediator*. Going to larger values of $g_{a\chi\chi}$, the ALPs are no longer in equilibrium with the SM, however due to the small value of g_{aff}, the chain of interactions SM$\to$ ALPs followed by $aa \to \chi\bar{\chi}$ dominates; and DM is said to be produced via *sequential freeze-in* (blue region in figure 1). Note here that, as the ALPs are not in equilibrium, their temperature is not well defined, such that the unintegrated Boltzmann equations are required [7]. This is beyond the scope of our work and we provide an estimate based on [4]. By further increasing $g_{a\chi\chi}$, the ALPs and DM particles enter into equilibrium before freeze-out at a temperature T' distinct from the visible sector temperature T. We will discuss this *decoupled freeze-out (DFO)* regime (red region in figure 1) in the following subsection. Finally, on the right side of the phase diagram all three sectors share a common temperature and DM is produced via thermal *freeze-out* (green region in figure 1).

4. Decoupled freeze-out

By solving the energy transfer Boltzmann equation for the energy density of the HS ρ':

$$\frac{\partial\rho'}{\partial t} + 3H\ (\rho' + P') = \int \frac{d^3p}{(2\pi)^3} C[f(p,t)], \tag{3}$$

we can determine the temperature T' which is related to ρ' via the equation of state. Note that the HS energy density is defined by $\rho' + P' = \rho_a + \rho_\chi + P_a + P_\chi$ in terms of the energy densities ρ_a, ρ_χ and pressures P_a, P_χ of the ALP a and DM χ respectively, H is the Hubble constant and

$C[f(p,t)]$ is the collision term, which accounts for the energy transfer via collisions to the HS. In our model, there are two differences from [3], the first is that the dominant contribution to the hidden sector energy is not from $f\bar{f} \to$HS but $f\bar{f} \to ag$, $gf \to af + f\bar{f} \to a$, which renders obtaining the collision term and solving the energy transfer Boltzmann equation more complicated, see the detailed discussion in [11]. The second is that we vary the expressions for the pressure and the energy density as a function of the temperature. Initially for $T' > m_\chi, m_a$ ALPs and DM are ultra-relativistic, $P' = \rho'/3$, and the universe is radiation-dominated, i.e. $\rho \propto T^4$, such that eq. (3):

$$\frac{\partial \rho'}{\partial t} + 4H\,\rho' = -H\left(T\frac{\partial \rho'}{\partial T} - 4\rho'\right) = -HT\rho\frac{\partial}{\partial T}\left(\frac{\rho'}{\rho}\right) = \int \frac{d^3p}{(2\pi)^3} C[f(p,t)]\,. \tag{4}$$

where $\rho' = \rho_a^{\rm eq}(T') + \rho_{\rm DM}^{\rm eq}(T')$ and $P' = P_a^{\rm eq}(T') + P_{\rm DM}^{\rm eq}(T')$, i.e. equilibrium distributions are assumed for both the ALPS and the DM. In this case one can simply solve this equation to obtain T'. For $T' \lesssim m_a, m_\chi$, the HS particles become non-relativistic, and interactions will freeze out, we define the energy density and pressure using:

$$\rho_\chi = \frac{\rho_\chi^{\rm eq}(T')}{n_\chi^{\rm eq}(T')}\, n_\chi\,, \qquad P_\chi = \frac{P_\chi^{\rm eq}(T')}{n_\chi^{\rm eq}(T')}\, n_\chi = T' n_\chi\,,$$

and similarly for the ALP. This introduces a dependence of the energy transfer Boltzmann equation on the number densities of the ALP and the DM. The hidden sector equation of state is then given by

$$\rho' + P' = \frac{\rho_\chi^{\rm eq}(T')}{n_\chi^{\rm eq}(T')}\, n_\chi + \frac{\rho_a^{\rm eq}(T')}{n_a^{\rm eq}(T')}\, n_a + T'\left(n_\chi + n_a\right)\,.$$

As a result, the Boltzmann equations for the number densities and the temperature T' must be solved as three coupled differential equations:

$$\begin{aligned}
z\frac{{\rm d}\rho'}{{\rm d}T'}\frac{{\rm d}T'}{{\rm d}z} &= -3(\rho' + P') + \frac{1}{H}\int \frac{d^3p}{(2\pi)^3} C[f(p,t)] \\
Hz\frac{{\rm d}n_\chi}{{\rm d}z} + 3Hn_\chi &= \sum_f \left\langle \sigma_{\chi\bar{\chi}\to f\bar{f}} v \right\rangle (T) n_\chi^{\rm eq}(T)^2 + \sum_{i,j,k} \langle \sigma_{\chi\bar{\chi} i\to jk} v^2 \rangle\, n_i^{\rm eq} \left(n_\chi^{\rm eq}\right)^2 \\
&\quad + \left\langle \sigma_{aa\to\chi\bar{\chi}} v \right\rangle (T') n_a^2 - \langle \sigma_{\chi\bar{\chi}\to aa} v \rangle\, (T') n_\chi^2 \\
Hz\frac{{\rm d}n_a}{{\rm d}z} + 3Hn_a &= \langle \Gamma_a \rangle\, n_a^{\rm eq}(T) + \sum_{i,j,k} \left\langle \sigma_{ia\to jk} v \right\rangle (T) n_a^{\rm eq}(T) n_i^{\rm eq}(T) \\
&\quad - \langle \sigma_{aa\to\chi\bar{\chi}} v \rangle\, (T') n_a^2 + \langle \sigma_{\chi\bar{\chi}\to aa} v \rangle\, (T') n_\chi^2
\end{aligned}$$

This is a stiff system of coupled differential equations, solving it is therefore non-trivial but can be accomplished using the stiff solver package dvode. The evolution of $Y_\chi \equiv n_\chi/s$ is tracked until the freeze out of the DM particles, i.e. until Y_χ stays constant. Note that, as for freeze-in, UV contributions to SM-DM and SM-ALP interactions can indirectly introduce a dependence on the reheating temperature via the energy transfer from the SM. We checked explicitly that for reheating temperatures below O(TeV) any effects on the the final DM relic abundance are small. To be more specific, varying $T_{\rm RH}$ from 200 GeV to 2000 GeV leads to a change of $\sim 22\%$ in the DM relic abundance and $\sim 7\%$ in the required value of $g_{a\chi\chi}$. We therefore neglect these. However, we do add finite-temperature corrections to both ALP and DM production from the SM, resulting in $O(1)$ corrections.

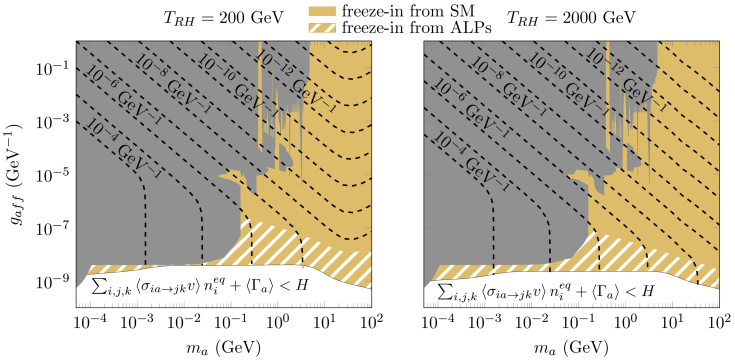

Figure 2: ALP-fermion coupling g_{aff} as a function of m_a for lines of constant hidden-sector coupling $g_{a\chi\chi}$ (plotted in dashed black) which reproduce the observed DM relic density via freeze-in from SM and freeze-in from ALPs as indicated for reheating temperatures $T_{RH} = 200$ GeV (left) and $T_{RH} = 2000$ GeV (right). We fixed the ratio $m_\chi/m_a = 10$. The lower line indicates the value of g_{aff} for which the ALPs and the SM reach equilibrium. In grey, we have included the relevant constraints on our ALP model on the connector coupling g_{aff} in this parameter region (cf. figure 1).

5. Results

Figure 1 summarises the beam dump, astrophysics and flavour physics bounds on ALPs which we calculated for our specific model, namely where the ALP only couples to SM fermions at tree-level and ALP-gauge boson couplings are induced by fermion loops. Astrophysical constraints coming from the neutrino burst from SN1987A or the ratio of the number of horizontal branch stars to red giants in globular clusters rely on energy loss arguments [9, 10]. The SLAC electron beam dump experiment searched for axions and observed no events [8]. For the flavour constraints, we derive bounds for the most constraining channels: $K^+ \to \pi^+ a(\to \text{inv.})$ from NA62, $K^+ \to \pi^+ a(\to \mu^+\mu^-)$ and $K^+ \to \pi^+ a(\to e^+e^-)$ from NA48/2, $B^+ \to K^+ a(\to \mu^+\mu^-)$ from LHCb and $B \to K^* a(\to \mu^+\mu^-)$ from LHCb and CHARM.

As discussed earlier, UV contributions to the DM relic density from a-mediated $2 \to 3$ scattering processes $f\bar{f} \to h\chi\bar{\chi}$, $fh \to f\chi\bar{\chi}$ and $\bar{f}h \to \bar{f}\chi\bar{\chi}$ become important for reheating temperatures above a few hundred GeV. These contributions introduce a dependence on the reheating temperature since the final relic abundance scales with T_{RH}, such that we consider two representative scenarios: $T_{RH} = 200$ GeV, where the UV contributions are almost negligible; the DM abundance will therefore be approximately independent of T_{RH} and $T_{RH} \sim 2000$ GeV, where the result is UV dominated. In figure 2 the yellow and yellow hatched regions depict the range in g_{aff} and m_a where the correct relic density is obtained, for different values of $g_{a\chi\chi}$, showing also contours for different values of the hidden sector coupling (dashed black lines) for these two scenarios. Inside the yellow region DM production from SM fermion scattering is more efficient (freeze-in from SM particles), and inside the yellow hatched region production from ALP scattering (freeze-in from ALPs). Note that for $T_{RH} = 200$ GeV and $m_\chi > m_t$, the Boltzmann suppression of the particles predominantly producing the DM via $t\bar{t} \to \chi\bar{\chi}$ results in an upwards bending of lines of constant hidden sector coupling. For the ultraviolet-dominated case, the lines of constant $g_{a\chi\chi}$ get shifted towards smaller values of g_{aff} since more DM is produced at earlier times. More details and

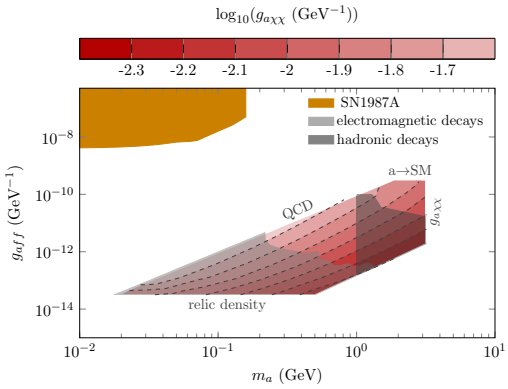

Figure 3: Contour plot of the hidden-sector couplings $g_{a\chi\chi}$ in the (m_a, g_{aff}) plane which give the observed DM relic density via decoupled freeze-out (DFO). We fixed the ratio $m_\chi/m_a = 10$. We have included the relevant constraints on our ALP model on the connector coupling g_{aff} in this parameter region (cf. figure 1). We additionally plot the region excluded by cosmological constraints of additional particles decaying electromagnetically (light grey) and decaying hadronically (dark grey). For explanations about the constraints from electromagnetic and hadronic decays see the main text.

discussion can be found in ref. [11].

In the DFO regime, contrary to the freeze-in regimes, $g_{a\chi\chi}$ is large to ensure equilibrium among the hidden sector particles. This can be seen in figure 3 where we show the region of parameter space where the correct relic density is obtained in the (m_a, g_{aff}) plane, again keeping the ratio $m_\chi/m_a = 10$ fixed, together with the constraints. Note that the boundaries of this region are described in [11]. One observes that it is challenging to test this region with collider searches for ALPs: in particular the SN bound and the bounds from rare B and K decays, would have to improve by several orders of magnitude. On the other hand, cosmology could test this region as the ALP is long-lived due to the tiny coupling between the SM particles and the ALP. Since the ALPs are abundantly produced along with the DM particles their decay has important implications for the cosmological history at the time of big bang nucleosynthesis. For ALPs with masses $m_a \lesssim 2m_\mu$, we apply the bounds from ref. [12] on very long-lived ALPs in the sub-GeV mass range, excluding lifetimes $\tau_a \sim 10^3 - 10^5$ s (bound labelled "electromagnetic decays"). For masses $2m_\mu \lesssim m_a \lesssim 1$ GeV, the ALP dominantly decays into muons, and here the lifetime is short enough for them not to matter. For hadronic decays the bounds become more severe and lifetimes above $\tau \sim 0.1$ s can be excluded [12] (bound labelled "hadronic decays"). More details can be found in ref. [11].

6. Conclusion

Our simple framework of an axion-like particle mediating DM leads to various alternative DM genesis scenarios. We calculated the relic density in the freeze-in and DFO regions, performing a detailed numerical calculation in an extensive region of the parameter space, where the calculation in the DFO regime was particularly non-trivial. For the freeze-in case the relic density is insensitive to the reheating temperature if it is below a few hundred GeV. We further presented brand-new

calculations of constraints on the ALP, in particular for SN, beam-dump and flavour constraints which were crucial for the parameter space of interest. Large regions in both the freeze-in and DFO regimes remain unexplored, and while the former could be probed by prospective collider experiments, the latter would be difficult to access. However, cosmology can help us constrain this region, and we have performed a first estimate of these bounds which should be improved in the future. Several further improvements to our analysis would also be advantageous: First we would like to improve the accuracy of our calculation in the sequential freeze-in region, by solving the unintegrated Boltzmann equation. Next we intend to analyse the thermal corrections in more detail. Finally we would like to perform a thorough assessment of the potential sensitivity of future experiments to the region of interest.

Acknowledgments

We are grateful to the organisers of the conference and our collaborators Felix Brümmer and Nishita Desai. This work was supported by the doctoral school ED352 and has received funding from the Excellence Initiative of Aix-Marseille University - A*MIDEX, a French "Investissement d'Avenir" programme (AMX-19-IET-008-IPhU).

References

[1] J. Quevillon and C. Smith, *Eur. Phys. J. C* **79**, 822 (2019).

[2] P. Gondolo and G. Gelmini, *Nuclear Physics B* **360**, 145–179 (1991).

[3] X. Chu, T. Hambye, M. H.G Tytgat, *Journal of Cosmology and Astroparticle Physics* **2012**, 34 (2012).

[4] T. Hambye and others, *Phys. Rev.* D **100**, 095018 (2019).

[5] L. Di Luzio and others, Phys. Rept. **870** (2020), 1-117 [arXiv:2003.01100 [hep-ph]].

[6] L. J. Hall and others, JHEP **03** (2010), 080 [arXiv:0911.1120 [hep-ph]].

[7] G. Bélanger and others, *Phys. Rev.* D **102**, 035017 (2020).

[8] J. D. Bjorken *et al*, *Phys. Rev.* D **38**, 3375–3386 (1988).

[9] J. H. Chang, R. Essig and S. D. McDermott, *Journal of High Energy Physics* **09**, 051 (2018).

[10] G. Raffelt and G. Starkman, *Phys. Rev.* D **40**, 942–947 (1989).

[11] A. Bharucha and others, JHEP **02** (2023), 141 [arXiv:2209.03932 [hep-ph]].

[12] M. Kawasaki and others, JCAP **12** (2020), 048 [arXiv:2006.14803 [hep-ph]]. Phys. Rev. D **97** (2018) no.2, 023502 [arXiv:1709.01211 [hep-ph]].